Study on the Deformation Impact of Shield Tunnel Overpass Construction on Existing Operational Tunnels

Song Chen[1],Zhenfeng Cao[1], Dexin Liu[2],Minglai Yang[1,3,*]
[1]Faculty of Intelligence Technology, Shanghai Institute of Technology, Shanghai, China
[2]Shanghai ShenTong Rail Transit Research and Consultancy CO., LTD., Shanghai, China
[3]College Of Information Technology, Jilin Agricultural University, Changchun, China

Abstract: Based on a shield-driven metro tunnel section in Shanghai, this paper systematically investigates the deformation characteristics and influence mechanism of overcrossing existing operational tunnels using the shield tunneling method. A three-dimensional finite element model (MIDAS GTS NX) was established, and a staged construction simulation method was adopted to analyze the deformation response of the existing tunnel during shield advancement, as well as the influence of tail synchronous grouting thickness on deformation control. The results indicate that the vertical deformation induced by shield tunneling exhibits significant phasing and symmetry. The left tunnel crossing induces a single-peak uplift response, whereas the right tunnel crossing evolves into an "M-shaped" double-peak pattern, with the peak deformation points shifting approximately 2.4 m from the centerline of the existing tunnel. Moreover, appropriately increasing the synchronous grouting layer thickness can effectively reduce deformation and improve the ground support capacity, with a 0.20 m thickness showing optimal performance in terms of deformation control and cost-effectiveness. The findings provide theoretical and engineering guidance for deformation control and risk management during shield tunneling under complex underground conditions.

Keywords: Overcrossing Existing Tunnel; Vertical Deformation Pattern; Synchronous Grouting Thickness

1. Introduction

This context underscores the importance of accurate predictive models and optimized construction strategies, particularly for shield tunnel crossings in dense urban environments.

With the rapid advancement of urbanization and the growing demand for underground space utilization, rail transit systems-owing to their high capacity, low land use, environmental friendliness, and efficiency-have been widely developed worldwide. As the core component of urban rail systems, metro networks are evolving towards deeper, more complex, and interconnected configurations.

Under the trend of increasing metro line density, constructing new tunnels that overcross existing operational tunnels has become a common yet technically challenging scenario. While shield tunneling offers advantages such as high efficiency and low disturbance, overcrossing operations still face critical challenges such as ground disturbance control, deformation management, and induced structural forces. These challenges are directly related to the safety and stability of existing tunnels and surrounding structures. To mitigate these risks, "Metro Safety Protection Zones" are typically delineated in practice, whereby shield crossings, excavation, and pile foundation works are subject to tiered supervision. This is supported by real-time monitoring and refined construction techniques to ensure deformation control, risk manageability, and operational safety throughout the construction process.

Numerous researchers have investigated close-proximity tunneling through field monitoring, theoretical analysis, numerical simulations, and physical modeling. Among them, Peck [1]developed an empirical formula based on extensive field data, using a Gaussian function to describe the surface settlement trough induced by shield excavation, which laid an important theoretical foundation for settlement prediction. Later studies refined this formula under varying geological conditions. For instance, Huang[2] et al. combined numerical simulation and the Peck formula to assess the impact of shield construction on existing structures and improve the accuracy of deformation prediction. Kun[3-5] et al. used numerical simulations combined with Peck's formula to propose a reference value for settlement trough width coefficient under soft soil conditions. Liao[6-8] et al. analyzed disturbance effects on operational tunnels and the surrounding

 Copyright @ STEMM Institute Press

environment using numerical simulations in metro over-underpass projects. Li[9-11] et al. conducted comparative analyses between simulation and field monitoring to examine deformation characteristics in overcrossing projects.

Current studies mostly focus on undercrossing or single-line overcrossing scenarios. However, there is relatively limited systematic research on double-line parallel tunnel overcrossings. This paper takes a section of a shield tunnel in the Shanghai metro system as a case study, establishing a 3D finite element model using MIDAS GTS NX to analyze the deformation responses of existing tunnels during the overcrossing process. The results aim to provide technical references and risk control guidance for similar complex tunneling projects.

2. Project Overview

2.1 Section Layout and Surrounding Environment

This project is located in Shanghai, within the shield tunnel section between two adjacent metro stations. After departing from one station, the new tunnel overpasses the existing tunnel, then passes beneath adjacent buildings and a substation. The section includes two cross passages and one pump station. The plan layout of the crossing route is shown in Figure 1.

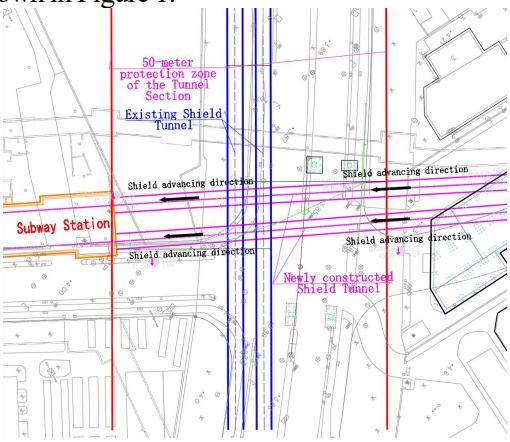

Figure 1. Schematic Diagram of Project Plan Position Relationship.

The new shield tunnel runs southeast to northwest, while the existing tunnel runs northeast to southwest, with the centerlines of the intersecting section nearly orthogonally arranged in plan view. At the overcrossing point, the track elevation of the existing tunnel is approximately -14.1 m. The minimum vertical clearance between the new and existing tunnels is about 1.0 m. The internal diameter of the existing tunnel is 5.9 m, with a ring width of 1.2 m, and it adopts a circular track slab structure. The section view of the project layout is shown in Figure 2.

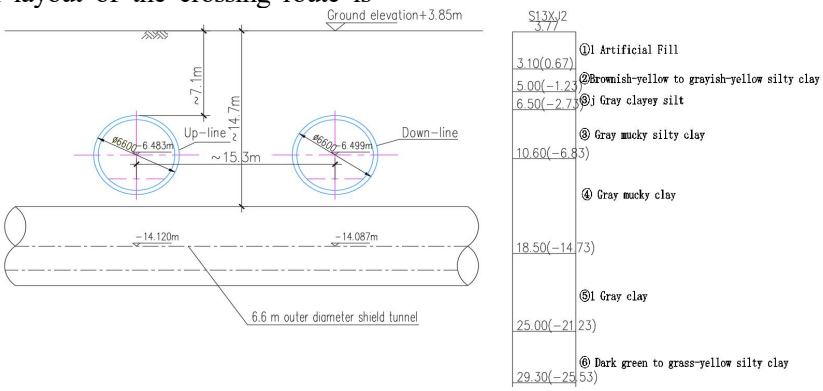

Figure 2. Schematic Diagram of Project Longitudinal Profile.

Based on spatial relations and construction disturbance characteristics, a 3D dynamic simulation model was built using MIDAS GTS NX. The model size is 70 m (length)×70 m (width)×35 m (height). Fine meshes (0.6 m) are used in the crossing area, 1.2 m meshes in the tunnel influence zone, and 1.4 m elsewhere. The mesh layout and shield crossing model are shown in Figures 3.

Both the soil and concrete segments are modeled using solid elements. The model contains 143,288 nodes and 244,236 elements. The Mohr-Coulomb model is used for soil, while the shield shell, segments, and grouting layer are modeled with elastic plate elements. The main parameters include an elastic modulus of 35.5 GPa for C55 concrete segments. The main material mechanical parameters are shown in Table 1.

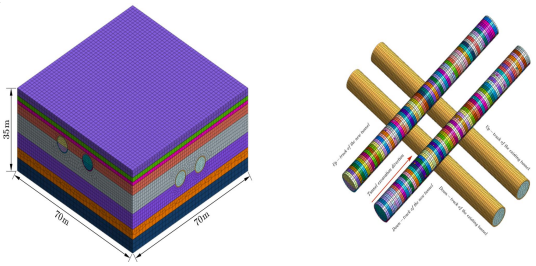

Figure 3. Grid Layout and Shield Machine Intersection Model

Copyright @ STEMM Institute Press

Table 1. Main Material Mechanical Parameters.

Material	Poisson's Ratio	Unit Weight (kN/m³)	Cohesion (KPa)	Friction Angle (°)	Elastic Modulus (MPa)
Fill	0.4	15	15	18	75
Brownish-yellow to grayish-yellow silty clay	0.35	18	20	19	20
Gray clayey silt	0.36	19	11	19	40
Gray mucky clayey silt	0.38	17.5	11.4	19	25
Gray mucky clay	0.4	18	13.6	12.7	20
Gray clay	0.38	19	15.8	18	25
Dark green to grass-yellow silty clay	0.36	20	45	17	40
Clayey silt interbedded with silty clay	0.38	23	7	29.5	90
shield shell	0.3	21			355000
segment	0.3	21			208000
grouting	0.4	21			32500

The numerical model adopts fully automatic boundary constraints to ensure computational stability and boundary responsiveness. The top surface of the model is set at ground level and defined as a free surface, thereby allowing vertical deformation to develop naturally without artificial boundary restrictions.

The shield tunneling load distribution is illustrated in Figure 4. The chamber pressure, applied at the tunnel face, is determined based on the detailed construction scheme and geological conditions, and is set to 0.15 MPa. This pressure simulates the support provided by the excavation chamber to maintain face stability during shield advancement.

The synchronous grouting pressure is applied around the segmental lining, oriented normally outward toward the surrounding soil. According to project-specific construction parameters and geotechnical properties, this pressure is also set to 0.15 MPa. The grouting layer thickness is assumed to be 0.20 meters, representing the annular gap backfilled during shield tail grouting.

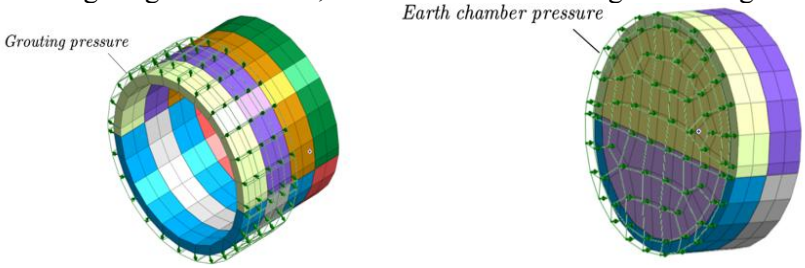

Figure 4. Schematic Diagram of Shield Tunneling Load Distribution

2.2 Simulation Method for Shield Tunnelling Construction

A staged excavation method is used to simulate the construction. The advancement and segment installation are simulated by activating/deactivating elements. Shield shell and grouting are modeled using attribute conversion. The simulation comprises 72 construction stages: 35 advancement segments for each tunnel line, with every two rings grouped as one analysis stage. Initial conditions activate soil and existing tunnel elements, and displacements are reset before excavation begins.

Key stages for the left and right tunnels are as follows:

Left Tunnel:

S4: Excavation of the first ring of the new tunnel's left line.

S9: First ring of tunnel segments produced; grouting pressure activated.

S14: Shield machine cutterhead enters existing tunnel right line.

S19: Shield machine cutterhead enters existing tunnel left line.

S21: Shield machine shield tail exits existing tunnel right line.

S26: Shield machine shield tail exits existing tunnel left line.

Right Tunnel:

S39: Excavation of the first ring of the new tunnel's right line.

S44: First ring of tunnel segments generated, grouting pressure activated.

S49: Shield machine cutterhead enters the existing tunnel's right line.

S54: Shield machine cutterhead enters the existing tunnel's left line.

S56: Shield machine shield tail exits the existing tunnel's right line.

S61: The shield machine's tail exits the existing

 Copyright @ STEMM Institute Press

tunnel's left line.

2.3.Simulation Results and Analysis

2.3.1.Left Tunnel Crossing

At construction stage S17, the shield advanced along the left line of the new tunnel and approached the boundary of the existing down-line tunnel. The excavation-induced stress relief in the surrounding soil led to ground disturbance, which in turn triggered deformation responses in the structure of the existing tunnel. At this stage, the shield was approximately 15 meters away from the existing up-line tunnel, resulting in significant vertical uplift of the down-line tunnel, with a maximum uplift value of 4.07 mm. In contrast, due to the greater distance, the up-line tunnel exhibited relatively minor deformation, with a maximum uplift of only 0.47 mm. The vertical deformation distribution of the existing tunnel at this stage is shown in Figure 5.

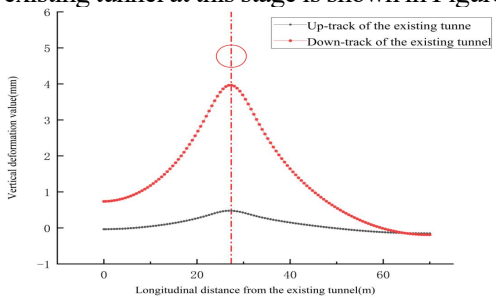

Figure 5. Vertical Deformation Profile of the Existing Tunnel At Stage S17.

At construction stage S27, the shield advanced such that the left line of the new tunnel completely crossed the existing up-line tunnel. At this point, both lines of the existing tunnel were affected by the shield crossing, and the overall deformation exhibited a general uplift trend. Compared with stage S17, the down-line tunnel experienced a slight reduction in maximum uplift, decreasing to 3.86 mm, due to partial rebound effects. In contrast, the up-line tunnel showed a further increase in uplift, reaching a maximum of 4.67 mm, as a result of the cumulative disturbance from dual crossing events. The vertical deformation distribution of the existing tunnel at this stage is presented in Figure 6.

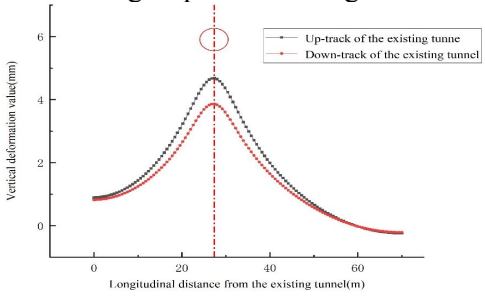

Figure 6. Vertical Deformation Profile of the Existing Tunnel at Stage S27.

2.3.2.Right Tunnel Crossing

At construction stage S50, the shield for the right line of the new tunnel advanced to the vicinity of the existing right-line tunnel boundary. The excavation-induced stress release in the surrounding soil triggered structural responses in the existing tunnel. Influenced by the inherent stiffness of the tunnel lining and its spatial configuration, the vertical uplift of the existing down-line tunnel exhibited a certain degree of lateral shift, and the deformation curve presented a characteristic "M-shaped" double-peak profile. The maximum uplift of the up-line tunnel reached 4.19 mm, while that of the down-line tunnel was 4.67 mm. The vertical deformation distribution at this stage is illustrated in Figure 7.

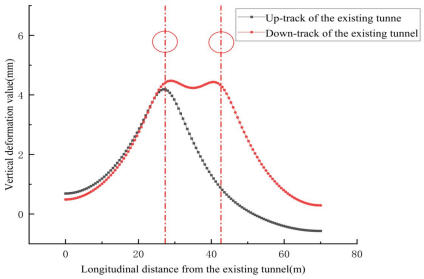

Figure 7. Vertical Deformation Profile of the Existing Tunnel at Stage S50.

At construction stage S61, the shield machine completed the crossing of both lines of the existing tunnel, and the deformation response further developed. The location of maximum vertical deformation of the existing tunnel shifted laterally from the original centerline, with a displacement of approximately 2.4 meters to either side. In addition, the vertical deformation on the side closer to the right line of the new tunnel was slightly greater, primarily due to the cumulative effect of the two successive tunnel crossings. The vertical deformation distribution at this stage is shown in Figure 8.

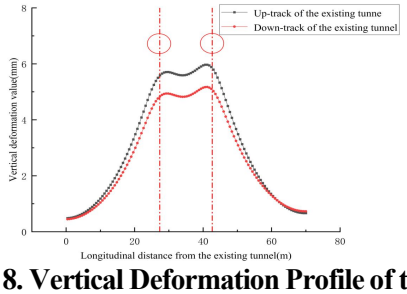

Figure 8. Vertical Deformation Profile of the Existing Tunnel at Stage S61.

2.3.3.Determining Optimal Grouting Thickness

During the upward crossing of existing tunnels by a shield-driven tunnel, controlling the vertical deformation of the existing structures is essential to ensuring construction safety and structural stability.

Copyright @ STEMM Institute Press

Tail void synchronous grouting, as a critical process that fills the gap between the shield shell and the segmental lining and maintains ground stability, plays a direct role in deformation control. The appropriate selection of grouting thickness and volume significantly affects the effectiveness of deformation mitigation.

To investigate the influence of grouting parameters on vertical deformation, this study conducts numerical simulations under consistent tunnelling conditions (Stage S61), considering three different synchronous grouting layer thicknesses: 0.15 m, 0.20 m, and 0.25 m. The simulation results are presented in Figure 9.

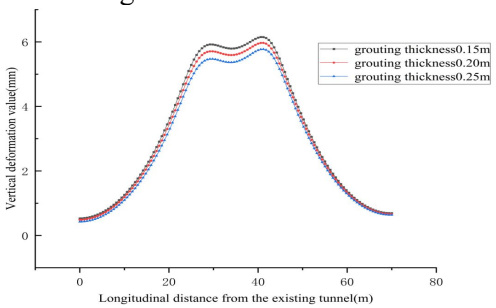

Figure 9. Effect of Grouting Thickness on Existing Tunnel Deformation at Stage S61.

The results indicate that as the grouting layer thickness increases, the maximum uplift above the existing tunnel gradually decreases, from approximately 6.3 mm to 5.5 mm, and the deformation curve becomes noticeably smoother. This demonstrates that a thicker grouting layer has a significant effect in mitigating excavation-induced disturbances and enhancing the arching support capacity of the surrounding ground. Considering both structural deformation control and construction cost-efficiency, a grouting thickness of 0.20 m provides a favorable balance and is recommended as the optimal design value for shield tunnelling operations in zones involving crossings over existing tunnels.

3. Conclusions

Focusing on the scenario of twin parallel metro tunnels in Shanghai crossing above an existing tunnel, this study systematically investigated the deformation behavior of the existing tunnel and the effectiveness of synchronous grouting control through three-dimensional numerical simulations. The main conclusions are as follows:

During the shield tunnelling process above the existing tunnel, the vertical deformation of the existing structure exhibits distinct stage-dependent characteristics. After the left-line crossing, the vertical displacement of the existing tunnel presents an approximately unimodal, normal distribution, with deformation concentrated and symmetrically distributed.

Upon completion of the right-line crossing, the deformation pattern transitions to a typical "M-shaped" double-peak curve, with the two peak points symmetrically offset by approximately 2.4 meters from the original centerline. Notably, the positions of these peaks remain stable during the subsequent construction stages.

The thickness of the synchronous grouting layer has a significant impact on the vertical deformation of the existing tunnel during shield overcrossing. As the grouting thickness increases, both the magnitude and spatial extent of uplift deformation gradually decrease. However, an excessively thick grouting layer does not yield proportional economic benefits. Therefore, it is recommended to flexibly determine the grouting thickness and volume based on deformation control requirements and construction feasibility.

References

[1]Peck, R.B. (1969) Deep Excavations and Tunneling in Soft Ground. Proc. of 7th ICSMFE, Mexico, 1969.

[2]Huang, J., et al. (2024) Evaluation Method of the Impact of Twin Shield Tunneling Construction on Elevated Bridges: Case Study. Symmetry-Basel, 16(9), 1113.

[3]Wang, K. (2017) Control Study on Subway Shield Tunneling Crossing Railway Subgrade in Ningbo Area. Journal of Railway Engineering, 34(4), 91-95.

[4]Liu, Y., Lei, H., Shi, L., Zheng, G. and Wang, M. (2025) Deformation Analysis of Ground and Existing Tunnel Induced by Overlapped Curved Shield Tunneling. Journal of Rock Mechanics and Geotechnical Engineering, 17(2), 795-809.

[5]Xu, Y., Zhang, Z., Zhang, C., Han, X., Liu, T. and Zhang, X. (2025) Analysis of Longitudinal Deformation of Existing Rectangular Pipe Jacking Tunnel Caused by Shield Tunnel Undercrossing. Tunnelling and Underground Space Technology, 161, 106532.

[6]Liao, S.M. and Yang, Y.H. (2012) Deformation Control and Measured Analysis of Shield Tunneling Crossing Existing Subway Tunnels. Chinese Journal of Geotechnical Engineering, 34(5), 812-818.

[7]Qi, Y., Hu, X., Zhou, S., Zhou, J., Wei, G., Zhang, D. (2024) Study on the effect of tunneling and secondary grouting on the deformation of existing pipelines in bedrock

 Copyright @ STEMM Institute Press

raised strata. Transportation Geotechnics, 45, 101218.

[8]Jiang, P. w., Zhang, Z. h., Zheng, H. and Huang, J. k. (2024) Coupling Analysis Method of Grouting Construction with Deformation Response of Adjacent Existing Tunnel. Underground Space, 15, 312-330.

[9]Li, J.-b., Zhao, M. and Tan, C. (2024) Safety Analysis of a New Tunnel Crossing Over an Existing Shield Tunnel. Geotechnical Foundation, 38(6), 913-920.

[10]Wang, Y., He, C., Zeng, D. y., and Su, Z. x. (2010) Model Test and Numerical Simulation of the Effect of Orthogonal Shield Tunnel Underpass Construction on an Existing Tunnel. Journal of the China Railway Society, 32(2), 79-85.

[11]Deng, L., Liu, J., Huang, C., Yang, S., Huang, J. and Wu, C. (2025) Impact of Twin Shield Tunnel Construction on the Deformation of Bridge Pile Groups beneath Multiple Bridges: A Case Study. Frontiers in Built Environment, 11, 1-15.

Copyright @ STEMM Institute Press